

Infrared and Ultraviolet Spectroscopy of Jet-Cooled *ortho*-, *meta*-, and *para*-Diethynylbenzene[†]

Jaime A. Stearns and Timothy S. Zwier*

Department of Chemistry, Purdue University, West Lafayette, Indiana 47907-1393

Received: April 30, 2003; In Final Form: August 22, 2003

The vibronic spectroscopy of *ortho*-, *meta*-, and *para*-diethynylbenzene (*o*DEB, *m*DEB, and *p*DEB) was studied by two-color resonant two photon ionization (R2PI). The symmetry allowed S_0 – S_1 origins of *o*DEB, *m*DEB, and *p*DEB were located at 33 515, 33 806, and 34 255 cm^{-1} , respectively, with the vibronic structure extending about 2000 cm^{-1} above the origin in *o*DEB and *m*DEB, but more than 3000 cm^{-1} in *p*DEB. Major peaks in each spectrum were attributed to vibronically induced bands, indicating strong coupling of the S_1 state to the S_2 state. Ground-state infrared spectra in the C–H stretch region (3000–3360 cm^{-1}) were obtained using resonant ion-dip infrared spectroscopy (RIDIRS). In all three isomers, the acetylenic C–H stretch fundamental was split by Fermi resonance with a combination band composed of the C≡C stretch and two quanta of the C≡C–H bend. This Fermi resonance was detuned in the overtone region of *p*DEB, which showed a single peak at 6556 cm^{-1} . Infrared spectra were also recorded in the excited electronic state using a UV–IR–UV version of RIDIR spectroscopy. In all three isomers, the acetylenic C–H stretch fundamental was unshifted from the ground state, but no Fermi resonance was seen. In addition to the sharp C–H stretch features, the *o*DEB S_1 infrared spectrum showed a broad absorption stretching from 3050 to 3250 cm^{-1} . Selective deuteration of *o*DEB at the acetylenic hydrogens led to infrared spectra that showed the broad absorption despite the absence of the acetylenic C–H stretch, indicating that the IR absorption is electronic in nature. Characteristics of this second excited state and its potential relevance as a gateway to a photochemical Bergman cyclization are discussed.

I. Introduction

The hydrogen abstraction– C_2H_2 addition (HACA) mechanism has been proposed as a route to polycyclic aromatic hydrocarbons (PAH) in flames.¹ Acetylated aromatic rings are therefore important combustion intermediates, although, in order to serve as a route to PAH, acetylation must be followed by ring closure. As Figure 1 shows, the formation of naphthalene from benzene via a HACA mechanism requires the addition of two acetylene molecules, with the styryl radical adduct (**3**) as a common intermediate. If the second C_2H_2 adds to the vinyl radical to form (**4**), subsequent attack of the diene radical on the ring leads to naphthalene (**9**).

In competition with this route is the loss of a hydrogen atom from (**3**) to form phenylacetylene (**5**). Subsequent abstraction of a ring hydrogen, followed by addition of a second C_2H_2 produces the disubstituted intermediate (**6a–c**). Loss of hydrogen from (**6**) produces *ortho*-, *meta*-, and *para*-diethynylbenzene (**7a–c**). Of these, only the *ortho* isomer can undergo Bergman cyclization² to form 1,4-dehydronaphthalene (**8**), which can add hydrogen to form naphthalene (**9**).

This is a notable example of a general issue in combustion models, which must explicitly incorporate the different reactivity of individual structural isomers. From an experimental point of view, the incorporation of isomer-specific chemistry requires isomer-specific detection, which by necessity must go beyond mass spectrometry to employ spectroscopic detection methods.

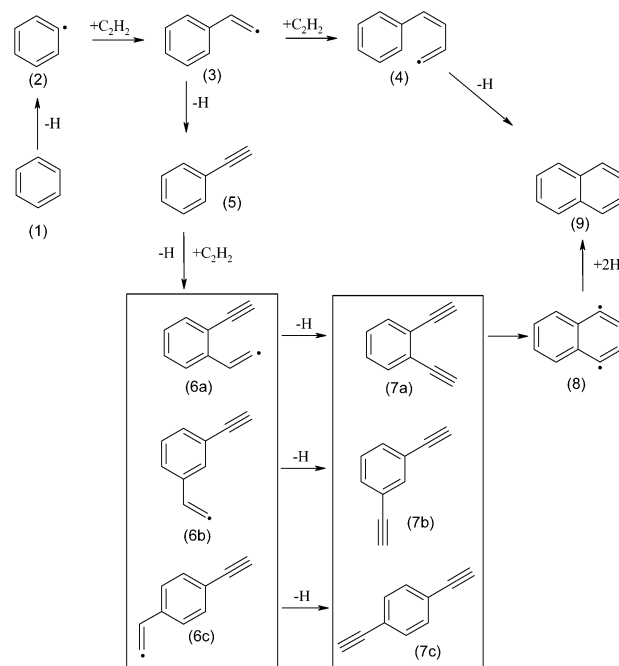


Figure 1. Schematic representation of the HACA mechanism for formation of naphthalene from benzene in acetylenic flames. Successive hydrogen atom abstraction and acetylene addition from benzene (**1**) leads to naphthalene via the radicals (**2**), (**3**), and (**4**). An alternative route is formation of phenylacetylene (**5**), the three diethynylbenzenes (**7a–c**), and, through Bergman cyclization, naphthalene (**9**).

A major purpose of this paper is to better characterize the electronic and ground- and excited-state vibrational spectroscopy

[†] Part of the special issue "Charles S. Parmenter Festschrift".

* To whom correspondence should be addressed. E-mail: zwier@purdue.edu. Phone: (765) 494-5278. Fax: (765) 494-0239.

of *ortho*-, *meta*-, and *para*-diethynylbenzene (**7a–c**). Previous spectroscopy of the three isomers of diethynylbenzene has been limited. Photoelectron spectroscopy³ established the ionization potentials of the *ortho*-, *meta*-, and *para* isomers to be 8.69, 8.82, and 8.58 eV respectively. The ground-state vibrational frequencies were determined by infrared and Raman spectroscopy in the liquid phase and in solution⁴ and, for *p*DEB, in the gas phase.⁵ The only electronic spectroscopy of the DEBs in the literature is the dispersed fluorescence spectrum of *p*DEB in a 77 K matrix.⁶ The $S_1(^1B_{2u})-S_0(^1A_g)$ origin in the matrix was assigned as 33 805 cm^{-1} . The spectrum was dominated by progressions built off of false origins of b_{3g} symmetry, indicating strong coupling between the $S_1(^1B_{2u})$ and $S_2(^1B_{1u})$ states. The S_1 origin of *p*DEB in the vapor phase was mentioned to be at 34 250 cm^{-1} although the rest of the spectrum was not discussed.

In the course of our study of the spectroscopy of *ortho*-diethynylbenzene, we have recorded infrared spectra of the molecule out of a series of S_1 vibronic levels, including the S_1 origin. These spectra reveal a broad absorption feature spread over the 3050–3250 cm^{-1} region that is not vibrational in character, raising the possibility that the absorption is linked to the photochemical Bergman cyclization of *o*DEB to the 1,4-dehydronaphthalene diradical (**8**). Although studies of the photochemical Bergman cyclization of *o*DEB are less prevalent, the thermal rearrangement has been well-characterized by both experiment and theory.^{7–9} Experiment has shown the barrier to cyclization to be 25.2 kcal/mol, with the ground-state diradical 17.8 kcal/mol above the *o*DEB ground state.⁷

Theoretical efforts to understand the photochemical cyclization have focused on the parent 3-hexen-1,5-diyne. Reaction along the first singlet excited potential energy surface was found to have a barrier similar to that of the ground-state reaction.¹⁰ Higher-lying states involving in-plane π excitations led to reaction pathways that were barrierless to excited states of the diradical.¹¹ However, no correlation between the excited states of a benzannelated enediyne such as *o*DEB and its corresponding diradical has appeared. Evenzahav and Turro¹² studied the photochemistry of alkyl-substituted *o*-diethynylbenzenes following near-UV excitation (~ 300 nm) in room temperature solution. Cyclization products were formed via a diradical intermediate in a process directly analogous to the thermal Bergman rearrangement. Our experiment excites *o*DEB in the same energy region, making the connection to the Bergman cyclization an intriguing possibility, which will be discussed.

II. Experimental Section

meta- and *para*-Diethynylbenzene were used as supplied (GFS Chemicals, each 98% purity). *ortho*-Diethynylbenzene was synthesized at Purdue University using a standard method.¹³ Acetylenic deuteration of *o*DEB was accomplished by stirring *o*-diethynylbenzene in hexanes with successive portions of D_2O in the presence of calcium oxide. The aqueous portion and hexanes were removed, and the remaining mixture of mono-, di-, and nondeuterated *o*-diethynylbenzene was used directly.

The experimental apparatus has been described previously.¹⁴ Briefly, diethynylbenzenes were introduced into the chamber by passing the buffer gas (~ 20 – 40 psig in He, N_2 , or Ne) over a reservoir of the sample and through a pulsed valve that produces 200 μs long gas pulses (R. M. Jordan Co.). The molecules were ionized 7 cm from the nozzle and detected by time-of-flight mass spectrometry.

Resonant two-photon ionization (R2PI) was used both to ionize the molecules and to obtain electronic spectra. Because of the high ionization potential of the diethynylbenzenes relative

to their $S_1 \leftarrow S_0$ origins, two-color R2PI was necessary. The first, resonant photon was provided by the frequency doubled output of a Nd:YAG pumped dye laser (270–300 nm). The source of the second, ionizing photon was either the fourth harmonic (266 nm) of a Nd:YAG laser (Continuum Minilite), or, when shorter wavelengths were required (up to 250 nm), the output of a Nd:YAG pumped LaserVision optical parametric converter and frequency doubler was used. A few tenths of a mJ/pulse were used for all UV sources.

Ground-state infrared spectra of the three isomers were acquired by resonant ion-dip infrared spectroscopy.¹⁵ In this experiment, the constant R2PI signal from a particular transition was monitored. When an infrared pulse resonant with a vibrational transition was introduced a few hundred nanoseconds before the R2PI lasers, the ground-state population was depleted. This depletion was observed as a dip in the R2PI signal, using active baseline subtraction in a gated integrator. Scanning the IR source provided a vibrational spectrum of the ground state.

We have also employed nonresonant ion-detected infrared (NIDIR) spectroscopy, a method developed by Fujii.¹⁶ The ultraviolet laser was tuned to a nonresonant wavelength (291.00 nm) chosen so that two UV photons are insufficient to ionize, but one infrared photon added to this energy exceeds the ionization threshold. Thus, the ion signal was recorded only when the infrared was resonant with a ground-state vibration. This method provided an excellent signal-to-noise ratio at the expense of the selectivity of double-resonance methods.

Infrared spectra of the excited states were obtained using a variation of RIDIRS. To probe the excited states, the resonant ultraviolet pulse arrived first, followed immediately by the infrared pulse, with the ionizing ultraviolet pulse last. The two UV lasers were typically separated by 40 ns. When the infrared pulse was resonant with a vibration in the excited state of the molecule, a portion of the population was excited by 3000 cm^{-1} or more, increasing the rate of nonradiative processes to vibrationally excited states of the electronic ground state. Because ionization is less efficient out of these states, a resonant transition was observed as a depletion in the ion signal. Scanning the IR frequency gave a vibrational spectrum of the excited electronic state.

The infrared source was a Nd:YAG pumped LaserVision optical parametric converter which provides tunable infrared light from 2000 to 4000 cm^{-1} with a power of a few mJ/pulse when the idler output is used and tens of mJ/pulse of 5000–7000 cm^{-1} when the signal beam is used. Selection of the signal or idler was accomplished by polarization selection at the output port.

Assignment of the spectra was assisted by calculations using Gaussian 98.¹⁷ Ground state geometries and frequencies were calculated by density functional theory with the Becke3LYP functional and a 6-31+G* basis set. The same basis set was used in CIS calculations to obtain excited state information. Because benzene derivatives undergo only minor geometry change in the first excited states, ground-state frequencies, scaled by 0.96, were used in analysis of the R2PI spectra.

III. Results and Analysis

A. R2PI Spectra. Figure 2a–c presents the two-color R2PI spectra of *para*-, *meta*-, and *ortho*-diethynylbenzene, respectively. The S_0-S_1 origins of *o*-, *m*-, and *p*-diethynylbenzene were found at 33 515, 33 806, and 34 255 cm^{-1} respectively. The intensity of the spectra decrease rapidly about 2000 cm^{-1} above the origin in *o*DEB and *m*DEB, probably due to decreased S_1 lifetime caused by an increased rate of nonradiative processes.

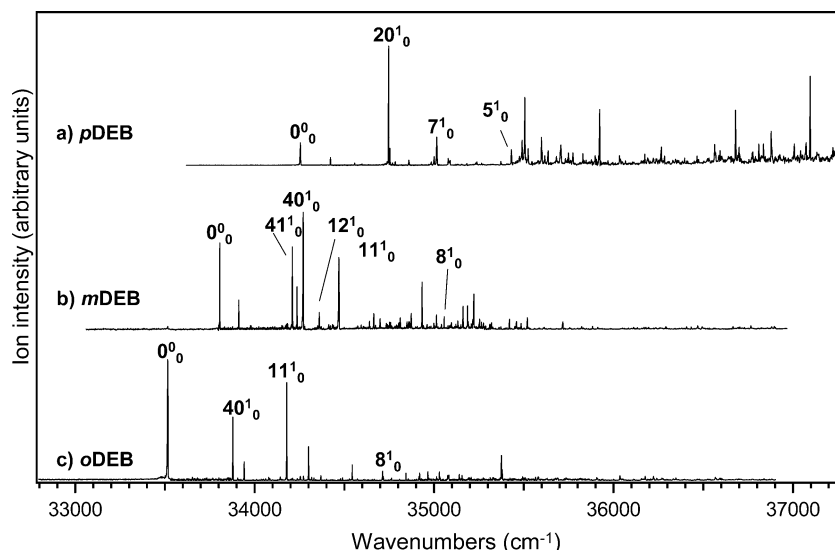


Figure 2. R2PI spectra of (a) *para*-, (b) *meta*-, and (c) *ortho*-diethynylbenzene, showing several assigned fundamentals. Numbering of vibrations is according to ref 4.

TABLE 1: Excited States of the Diethynylbenzenes Predicted by CIS/6-31+G*

isomer (symm)	state (exp S_n) ^a	calc energy (eV)	calc S_0 - S_n osc. strength	transition moment directions from ground state to labeled upper state
<i>para</i> (D_{2h})	${}^1B_{1u}$ (S_2)	5.08	0.59	
	${}^1B_{2u}$ (S_1)	5.65	0.01	
<i>meta</i> (C_{2v})	1A_1 (S_2)	5.35	0.10	
	1B_2 (S_1)	5.61	0.002	
<i>ortho</i> (C_{2v})	1B_2 (S_2)	5.17	0.16	
	1A_1 (S_1)	5.58	0.02	

^a Assignment of the state to S_1 or S_2 is based on experimental evidence (see text). In all cases, the experimental ordering is the reverse of that predicted by CIS.

1. para-Diethynylbenzene. Of the three isomers, the S_0 - S_1 origin is weakest in *p*DEB. Following Laposa,⁶ this transition is assigned as $S_1({}^1B_{2u}) \leftarrow S_0({}^1A_g)$, with an allowed transition moment pointing perpendicular to the substitution axis (Table 1). This is consistent with the corresponding S_0 - S_1 transitions in phenylacetylene¹⁸ and *para*-difluorobenzene.¹⁹

The weak intensity of the origin transition and the strong vibronic structure built off of it could reflect a large geometry change accompanying electronic excitation. However, this would result in long Franck-Condon progressions in vibrations that map along the direction of the structural change, and such progressions are not observed. Instead, the dominant transition

in the spectrum, which occurs 492 cm^{-1} above the origin, does not have observable intensity in transitions to $\nu > 1$. This band is thus a false origin arising from vibronic coupling involving a nontotally symmetric fundamental. We assign the band at 492 cm^{-1} to 20^1_0 , where ν_{20} is a b_{3g} C-C≡C bend. Its appearance in the spectrum indicates that intensity borrowing is occurring from the $S_2({}^1B_{1u})$ state. This assignment is in keeping with the analogous assignments given by Laposa⁶ in the dispersed emission spectrum of the molecule in a 77 K matrix (where 20^0_1 appears at 535 cm^{-1}) and with the corresponding mode, ν_{35} , in the phenylacetylene S_0 - S_1 spectrum.¹⁸

CIS calculations (Table 1) correctly identify the presence of two close-lying excited singlet states, but predict their energy ordering incorrectly, placing the B_{1u} state, with its large oscillator strength, lower in energy than the weakly allowed B_{2u} state. The CIS calculations do correctly predict the large difference, a factor of nearly 60, in the oscillator strengths of the first two excited states. This reordering of states has been previously discussed for phenylacetylene²⁰ and several isomers of divinylbenzene.²¹

Once the importance of vibronic coupling with the S_2 state is recognized, much of the observed vibronic structure can be rationalized in terms of transitions involving three normal modes: $\nu_5(a_g)$, $\nu_7(a_g)$, and $\nu_{20}(b_{3g})$. As shown in Figure 2a and summarized in Table 2, totally symmetric fundamentals 7^1_0 and 5^1_0 appear at 760 and 1176 cm^{-1} , with weak overtones appearing at twice these frequencies. The corresponding bands appear built off of 20^1_0 at 1250 ($492+758$) and 1668 ($492+1176$) cm^{-1} . Transitions at 605 and 1452 cm^{-1} are tentatively assigned to a_g modes 18^1_0 and 4^1_0 .

We do not have a firm assignment for the band appearing 168 cm^{-1} above the S_0 - S_1 origin. This band could be either a low frequency totally symmetric fundamental, a b_{3g} fundamental appearing by virtue of vibronic coupling, or an overtone of a nontotally symmetric fundamental. Of these possibilities, the low frequency of the band suggests an assignment as the b_{3g} fundamental 21^1_0 , which is calculated to have a frequency of 178 cm^{-1} in S_0 , and may lower its frequency still further in S_1 .

2. meta-Diethynylbenzene. As in *p*DEB, the S_0 - S_1 R2PI spectrum of *m*DEB (Figure 2b) exhibits peaks more intense than the origin without long progressions in these modes. These bands must be assigned to nontotally symmetric vibrations that gain intensity by borrowing from the nearby S_2 state. The identities

TABLE 2: Assignments for Major Peaks in the R2PI Spectra of the Diethynylbenzenes

description	<i>p</i> DEB				<i>m</i> DEB				<i>o</i> DEB			
	frequencies (cm ⁻¹)		symm	mode ^{c,d}	frequencies (cm ⁻¹)		symm	mode ^{c,d}	frequencies (cm ⁻¹)		symm	mode ^{c,d}
exp ^a	calc ^b	exp ^a			calc ^b	exp ^a			calc ^b			
C–X bend	168	178	b _{3g}	(21 ¹ ₀)	106	180	b ₂	(42 ¹ ₀)				
C–X stretch					405	450	b ₂	41 ¹ ₀	363	407	b ₂	40 ¹ ₀
C–X wag or C≡C–C bend					430	445,	a ₁	(14 ¹ ₀ ,	427	541,	a ₁	(13 ¹ ₀ ,
C≡C–C bend						481		13 ¹ ₀)		441		14 ¹ ₀)
C≡C–H bend	492	530	b _{3g}	20 ¹ ₀	465	553	b ₂	40 ¹ ₀				
ring C–C	605	636	b _{3g}	(18 ¹ ₀)	555	621	a ₁	12 ¹ ₀				
ring breathe	760	789	a _g	7 ¹ ₀	664	688	a ₁	11 ¹ ₀	664	693	a ₁	11 ¹ ₀
C–X stretch	1176	1180	a _g	5 ¹ ₀	1251	1217	a ₁	8 ¹ ₀	1198	1184	a ₁	8 ¹ ₀
ring C–C	1452	1588	a _g	(4 ¹ ₀)								
combination bands	frequency (cm ⁻¹)		mode		frequency (cm ⁻¹)		mode		frequency (cm ⁻¹)		mode	
		1250		7 ¹ ₀ 20 ¹ ₀		834		430+41 ¹ ₀		785		427+40 ¹ ₀
		1343		5 ¹ ₀ 8 ¹ ₀		858		430 × 2		1029		11 ¹ ₀ 40 ¹ ₀
		1519		7 ² ₀		894		430+40 ¹ ₀		1328		11 ² ₀
		1668		5 ¹ ₀ 20 ¹ ₀		1006		12 ¹ ₀ 41 ¹ ₀		1451		427+11 ¹ ₀ 40 ¹ ₀
		1779		5 ¹ ₀ 18 ¹ ₀		1067		11 ¹ ₀ 41 ¹ ₀		1515		427 × 2+11 ¹ ₀
		2012		7 ² ₀ 20 ¹ ₀		1128		11 ¹ ₀ 40 ¹ ₀		1625		427+8 ¹ ₀
		2211		4 ¹ ₀ 7 ¹ ₀		1654		8 ¹ ₀ 41 ¹ ₀		1860		8 ¹ ₀ 11 ¹ ₀
		2425		5 ¹ ₀ 7 ¹ ₀ 20 ¹ ₀		1714		8 ¹ ₀ 40 ¹ ₀				
		2518		5 ² ₀ 8 ¹ ₀		1912		8 ¹ ₀ 11 ¹ ₀				
		2628		4 ¹ ₀ 5 ¹ ₀								
		2841		5 ² ₀ 20 ¹ ₀								

^a Experimental frequency, measured from the origin. ^b Ground-state frequency calculated using B3LYP/6-31+G* and scaled by 0.96. ^c Numbering according to ref 4. ^d Assignments in parentheses are tentative.

of the excited electronic states can be assigned by consideration of CIS results and by analogy to *p*DEB. CIS calculations find two low-lying π - π^* states, one each of A₁ and B₂ symmetry (Table 1). The presence of intense vibronically induced structure in the spectrum implies that the transition with the lower oscillator strength (¹B₂) is to the lower energy state, as was the case with *p*DEB. We therefore tentatively assign the S₀–S₁ transition as ¹A₁–¹B₂, with the transition moment pointing perpendicular to the C₂ axis (Table 1). This assignment is consistent with that deduced from the fully rotationally resolved spectra for the *meta*-divinylbenzenes by Nguyen et al.²¹

Much of the structure in the *m*DEB R2PI spectrum can be assigned using the same vibrational modes found in the corresponding *p*DEB and phenylacetylene¹⁸ spectra. The largest peak in the *m*DEB spectrum (465 cm⁻¹) is assigned to 40¹₀, where ν_{40} is the same C–C≡C bend as ν_{20} in *p*DEB. The other false origin at 405 cm⁻¹ is assigned to 41¹₀, a substituent-sensitive stretch. Two bands in *m*DEB (11¹₀ at 664 cm⁻¹ and 8¹₀ at 1251 cm⁻¹) are assigned to the same totally symmetric vibrations as those that dominate the *p*DEB spectrum.

Three other transitions are assigned as totally symmetric fundamentals. Considering the ground-state frequencies and the fact that most vibrations of phenylacetylene are red-shifted in the excited state,¹⁸ the peak at 430 cm⁻¹ is either a substituent wagging vibration (14¹₀) or the C–C≡C bend (13¹₀). The peak at 555 cm⁻¹ is assigned by the same logic to the CCH bend (12¹₀). By analogy to *p*DEB, the peak located 106 cm⁻¹ above the origin is tentatively assigned to 42¹₀, where ν_{42} is a C–X wag. Much of the remaining structure in the *m*DEB R2PI spectrum, listed in Table 2, is made up of combination bands of the modes already discussed.

3. *ortho*-Diethynylbenzene. *o*DEB is calculated to have excited electronic states closely analogous to those of the other two DEB isomers. The presence of strong vibronic bands (vide infra) in the R2PI spectrum (Figure 2c) indicates that the S₂ state once again carries greater oscillator strength than S₁, leading us to

conclude that CIS calculations again reverse the first two excited states (Table 1). The observed transition is assigned to S₀(¹A₁)–S₁(¹A₁) with a transition moment parallel to the C₂ axis. Note that, although the S₁ states in *o*DEB and *m*DEB have different symmetry designations, the nodal patterns on the ring are the same. As was noted for *ortho*- and *meta*-difluorobenzene, the symmetry of the upper state depends on whether the C₂ axis passes through atoms (*meta*) or through bonds (*ortho*).²²

The R2PI spectrum of *o*DEB contains a peak 363 cm⁻¹ above the origin, which can be assigned as a vibronically induced band (40¹₀). Two bands (11¹₀ at 664 cm⁻¹ and 8¹₀ at 1198 cm⁻¹) can be assigned to totally symmetric ring breathing and substituent-sensitive stretching present in the other isomers. The peak at 427 cm⁻¹ is likely the same mode as that at 430 cm⁻¹ in *m*DEB. Again, much of the remaining structure is understood in terms of combinations of the four modes mentioned here (Table 2).

A comparison of the spectra of the three isomers uncovers some differences in their spectroscopy. In particular, the *o*DEB isomer is missing a second, strong vibronic band observed in the *meta* isomer. It also lacks a low frequency vibronic band that is clearly observed in the other two isomers (<200 cm⁻¹). These differences likely reflect differences in the vibronic coupling matrix elements involving the various in-plane vibrations of the three isomers. In addition, there may be differences in Franck–Condon factors involving totally symmetric levels due to changing nodal patterns in the π - π^* transitions of the three isomers.

B. Ground-State Infrared Spectra. Figure 3a–c presents the ground electronic state RIDIR spectra of *para*-, *meta*-, and *ortho*-diethynylbenzene, respectively. The spectra span the aromatic and acetylenic C–H stretch regions, though the aromatic C–H stretch transitions are just barely visible in the region between 3050 and 3100 cm⁻¹. Because of extensive Fermi resonance mixing, the aromatic C–H stretch fundamentals are notoriously difficult to assign and will not be considered further here.

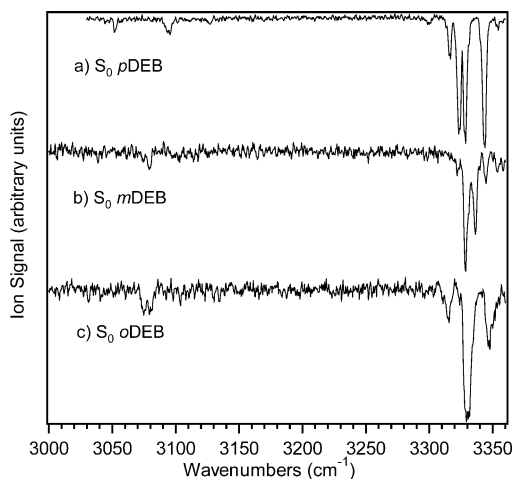


Figure 3. Ground-state RIDIR spectra of (a) *p*-, (b) *m*-, and (c) *o*-diethynylbenzene in the aromatic and acetylenic C–H stretching region. The numerous peaks above 3300 cm^{-1} are attributed to Fermi resonance. See the text for further discussion.

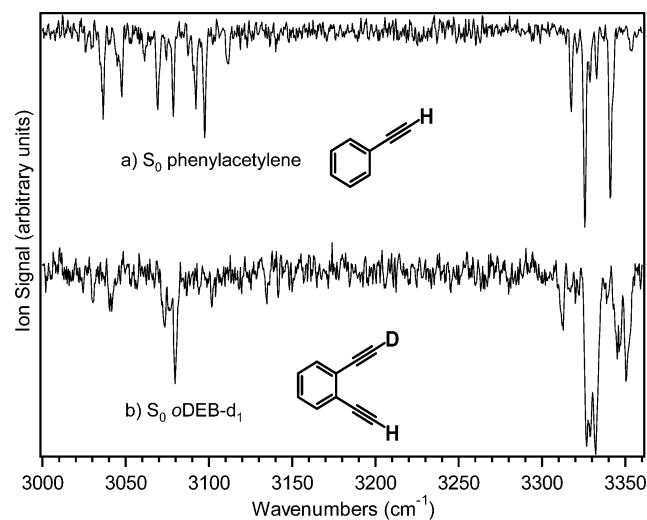


Figure 4. Ground-state RIDIR spectra of (a) phenylacetylene and (b) *ortho*-diethynylbenzene- d_1 , two molecules similar to the diethynylbenzenes but possessing only a single acetylenic substituent. The acetylenic C–H stretch region shows the numerous peaks created by Fermi resonance mixing.

The most intense transitions in the spectra are due to the acetylenic C–H stretch fundamental(s), which appear as clusters of transitions near 3330 cm^{-1} . The complexity of the acetylenic C–H stretch region in the diethynylbenzene spectra indicates the presence of Fermi resonance mixing, a well-documented phenomenon arising from the interaction of the acetylenic C–H stretch with a combination band composed of two quanta of the acetylenic C–H bend and the C≡C stretch.²³ In an attempt to better understand the nature of the Fermi resonances in these isomers, we have also recorded RIDIR spectra of two related molecules with single acetylenic C–H stretch fundamentals: phenylacetylene and *ortho*-diethynylbenzene- d_1 . These are shown in Figure 4, parts a and b, respectively.

1. Phenylacetylene. The acetylenic C–H stretch region of phenylacetylene’s vapor phase infrared spectrum has been previously characterized at room temperature as an intense peak around 3340 cm^{-1} and a shoulder at 3320 cm^{-1} assigned respectively as the single C–H stretch fundamental and a combination band composed of one quantum of the C≡C stretch (2120 cm^{-1}) and two quanta of the out-of-plane C≡C–H bend (fundamental at 613 cm^{-1}).^{23,24} In the supersonic expansion,

TABLE 3: Frequencies that May Be Involved in the Ground State Fermi Resonance of *p*-Diethynylbenzene

mode ^a	description	symm	calc freq (cm ⁻¹) ^b	exp freq (cm ⁻¹) ^a
ν_{24}	CH stretch	b_{1u}	3344	3305
ν_3	C≡C stretch	a_g	2117	2108
ν_{26}	C≡C stretch	b_{1u}	2122	2110
ν_{12}	oop CH bend	b_{2g}	569	618
ν_{19}	ip CH bend	b_{3g}	621	632
ν_{35}	ip CH bend	b_{2u}	622	646
ν_{39}	oop CH bend	b_{3u}	572	615
combination bands	$\nu_3 + \nu_{12} + \nu_{39}$		3258	3341
	$\nu_{26} + 2\nu_{12}$		3260	3346
	$\nu_{26} + 2\nu_{39}$		3266	3340
	$\nu_3 + \nu_{19} + \nu_{35}$		3360	3386
	$\nu_3 + 2\nu_{35}$		3361	3400
	$\nu_{26} + 2\nu_{19}$		3364	3374

^a Reference 4. ^b Calculated at the B3LYP/6-31+G* level of theory and scaled by 0.96.

these peaks are fully resolved and appear at 3341 and 3326 cm^{-1} , along with a smaller peak at 3318 cm^{-1} (Figure 4a).

Although it is possible that the resonant combination band might involve in-plane bends, these appear higher in frequency (fundamental at 640 cm^{-1})²⁴ giving rise to a combination band that would appear at 3418 cm^{-1} , much higher than the observed transitions. However, the DFT calculations predict the bending vibrations to be at 621 (in-plane) and 566 cm^{-1} (out-of-plane), implying that the in-plane bends would be better candidates for Fermi resonance. We attribute the difference between calculation and experiment to the imperfect practice of scaling calculated frequencies by a single scale factor irrespective of the type of vibration. In keeping with the previous assignments,^{23,24} we attribute the intense Fermi resonance band to the combination band involving out-of-plane bends, whereas the smaller peaks in the spectrum may be due to higher order couplings that are enhanced in size by the partial saturation inherent to depletion spectroscopy.

2. *para*-Diethynylbenzene. Because only a single acetylenic C–H stretch fundamental is symmetry allowed in the IR spectrum of *p*DEB, three of the four intense peaks in Figure 3a must be ascribed to Fermi resonance. There are six combinations of modes that can be in Fermi resonance with the antisymmetric C–H stretch (Table 3), which are grouped according to the nature (in-plane or out-of-plane) of the C≡C–H bends involved. Frequencies from the DFT calculations indicate the higher frequency group matches better with the calculated C–H stretch fundamental, whereas frequencies observed in the solution phase⁴ indicate the lower frequency group would be in resonance with the C–H stretch. As with phenylacetylene, our calculations likely underestimate the bending frequencies, so we tentatively assign the Fermi resonance mixing in *p*DEB to out-of-plane rather than in-plane C≡C–H bends. The absence of Fermi resonance in the solution-phase diethynylbenzene spectra can be explained by the sensitivity of the C–H stretch fundamental to its environment. For *p*DEB in solution, this vibration was shifted down to 3305 cm^{-1} .⁴

Often in circumstances where Fermi resonances contribute to the spectrum of a fundamental, further insight can be gained by following the effects of the Fermi resonance into the overtone region.²⁵ Figure 5 presents a close-up of the first overtone acetylenic stretch region of *p*DEB recorded using NIDIR (Figure 5a) and RIDIR (Figure 5b) spectroscopy. The signal beam from the infrared parametric converter was used for this purpose. The spectra exhibit a single transition at 6556 cm^{-1} , indicating that the Fermi resonances that appear in the fundamental are tuned

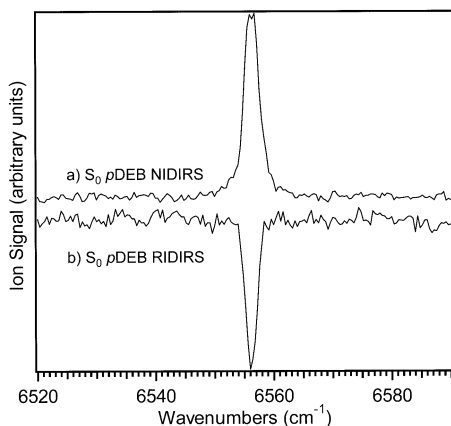


Figure 5. Ground-state (a) NIDIR and (b) RIDIR spectra of the acetylenic C–H stretch overtone of *para*-diethynylbenzene. The single peak at 6556 cm^{-1} shows that the anharmonicity of the C–H stretch removes the Fermi resonance that is so strong in the fundamental region.

out of resonance at the first overtone, probably due to the $\sim 50 \text{ cm}^{-1}$ anharmonicity of the C–H stretch.

3. *meta*-Diethynylbenzene. The *m*DEB RIDIR spectrum is composed of two large peaks and two small peaks in the acetylenic C–H stretch fundamental region. Both the a_1 and b_2 symmetry fundamentals are allowed, and both are calculated to have significant intensity. The relative frequencies and intensities of the two most intense peaks in the spectrum (3328 and 3336 cm^{-1}) are consistent with assignments to the b_2 and a_1 fundamentals, respectively. Interestingly, it appears that Fermi resonance plays a smaller role in the meta isomer than it does in the others. *meta*-Diethynylbenzene has C \equiv C stretch, C \equiv C–H stretch, and C \equiv C–H bending vibrations close in frequency to those of *para*-diethynylbenzene, with similar symmetry restrictions on which combinations can mix with the two acetylenic C–H stretch fundamentals. However, the presence of Fermi resonance is not as obvious in *m*DEB as in *p*DEB, appearing only in the small peaks to either side of the fundamentals. It is possible that meta substitution creates smaller kinetic coupling between the two substituents, thereby minimizing the strength of the Fermi coupling in this case.

4. *ortho*-Diethynylbenzene and *ortho*-Diethynylbenzene- d_1 . The *ortho* isomer has one very broad peak with smaller broadened peaks flanking it on either side (Figure 3c). As in the meta isomer, both symmetric and antisymmetric acetylenic C–H stretch fundamentals are calculated to carry significant intensity, so both contribute to the spectrum along with one or more states gaining intensity by Fermi resonance mixing with the acetylenic C–H stretch fundamentals. Without resolving the broad peaks in this spectrum, no firm assignments can be made.

The RIDIR spectrum of *o*-diethynylbenzene- d_1 (Figure 4b) exhibits two doublets and a smaller peak, confirming that the broad peaks in the undeuterated species are composed of a number of peaks that are not resolvable. The two spectra in Figure 4 are very similar, with each of the transitions in phenylacetylene (Figure 4a) split into doublets with a separation of 5.2 cm^{-1} in *o*DEB- d_1 (Figure 4b). We do not have an explanation for this further splitting.

C. S_1 -State RIDIRS. In the course of recording two-color R2PI spectra, the S_1 excited-state lifetimes of *o*-, *m*-, and *p*DEB were determined to be approximately 20 ns. This was sufficiently long that infrared spectra of the S_1 state could be recorded using RIDIR methods as described in section II. Figure 6a–c shows the S_1 -state RIDIR scans of *para*-, *meta*-, and *ortho*-diethynylbenzene out of their respective S_1 zero-point levels.

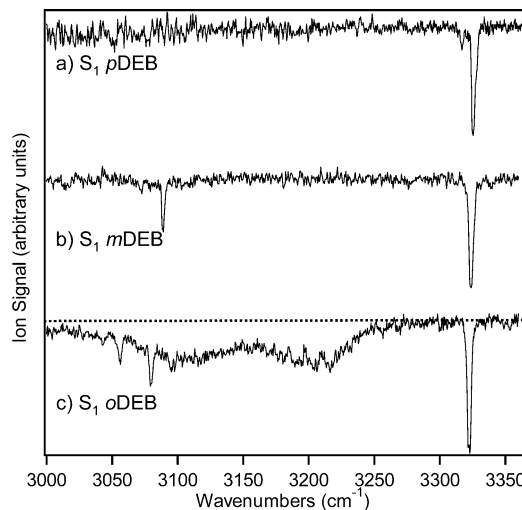


Figure 6. Excited-state RIDIR spectra of (a) *para*-, (b) *meta*-, and (c) *ortho*-diethynylbenzene in the aromatic and acetylenic C–H stretching region. The Fermi resonances above 3300 cm^{-1} are no longer present in the excited state, but the *o*DEB spectrum is dominated by a broad absorption from 3050 to 3250 cm^{-1} .

The aromatic C–H stretch transitions appear in the same region as the ground state, with modest shifts from their ground-state values. The spectra each show one significant peak in the acetylenic C–H stretch region, at 3323, 3324, and 3325 cm^{-1} for *o*-, *m*-, and *p*DEB, respectively. Only the *para* isomer shows any trace of the Fermi resonances that are present in the ground state, with an additional weak transition at 3317 cm^{-1} . Because the fundamental acetylenic C–H stretch appears in nearly the same position in the ground and excited states, the lack of Fermi resonance in S_1 must be attributed to a shift in frequency of the other modes. The C \equiv C stretch, for instance, is known to be 100 cm^{-1} lower in S_1 than in the ground state in phenylacetylene.¹⁸

The most striking aspect of the S_1 -state spectra is the broad, double-humped absorption that appears in the spectrum of *o*DEB, spread over the 3050–3250 cm^{-1} region. No similar feature was seen in either the *para*- or *meta*- isomers or in any other part of the *o*DEB spectrum from 2600 to 3600 cm^{-1} .

The broad absorption is suggestive of an infrared transition due to a weakened acetylenic C–H stretch fundamental. However, this feature appears in addition to the acetylenic C–H stretch transition, rather than replacing it, and would imply a 10-fold increase in the intensity of the transition. Similarly, attribution of the broad absorption to a blue-shifted aromatic C–H stretch would require a 100-fold increase in the C–H stretch intensity.

In an attempt to isolate the source of this unique absorption, the dependence of the spectrum on several key experimental parameters was tested. First, a series of S_1 RIDIR spectra were recorded using S_1 vibronic levels 364, 1030, and 1860 cm^{-1} above the S_1 origin as the intermediate state. These spectra showed only modest changes in the frequency range and shape of the broad absorption. Second, the wavelength of the ionization laser was changed over the 250–270 nm region with no apparent effect on the spectrum. Third, several scans were recorded with varying delays between the UV excitation, infrared, and ionization laser pulses. In all cases, the ionization signal that was depleted by the infrared pulse followed the S_1 -state lifetime ($\tau \sim 22 \text{ ns}$). Furthermore, the intensity and shape of the broad absorption did not change relative to the sharp C–H stretch as the timing of the infrared relative to the other two lasers was varied. This rules out the possibility that part of the ion signal,

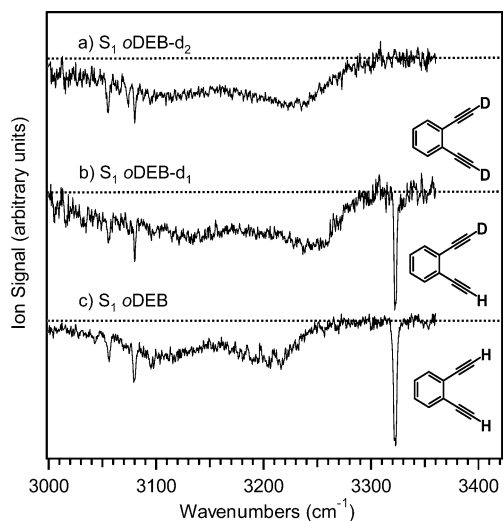


Figure 7. Excited-state RIDIR spectra of (a) dideuterated, (b) monodeuterated, and (c) undeuterated *o*-diethynylbenzene in the aromatic and acetylenic C–H stretching region. Despite the absence of the C–H stretch fundamental in *o*DEB- d_2 , the broad absorption is still present, indicating it is an electronic transition.

and therefore the broad absorption, arises from a long-lived species (e.g., a triplet state).

A final and most conclusive test involved recording the excited-state infrared spectra of the *o*DEB- d_1 and *o*DEB- d_2 isotopomers, deuterated at the acetylenic C–H groups. As shown in Figure 7, parts a and b, respectively, both the d_2 and d_1 *o*DEB isomers possess the same broad absorption that characterized the d_0 species (reproduced in Figure 7c). The presence of this absorption in the di-deuterated species, even though the sharp acetylenic C–H stretch is missing, clearly indicates that the infrared absorption is not associated with a modified C–H stretch fundamental but instead must be ascribed to a relatively weak electronic transition.

IV. Discussion

A. Diethynylbenzenes in the HACA Scheme. The HACA mechanism provides a potential pathway from benzene to naphthalene. However, as Figure 1 shows, there are routes that deviate from this pathway. The meta and para isomers of diethynylbenzene are two examples of species that may be thought of as sinks which trap population in pathways other than those that lead to additional ring formation. The ortho isomer may form naphthalene, but it may also continue the hydrogen-abstraction– C_2H_2 -addition process to form other species that prohibit PAH formation. Further insight into the role of the diethynylbenzenes in acetylenic flames may be gained by doping the diethynylbenzenes into acetylenic flames.²⁶

More generally, the present data provides a spectroscopic foundation for distinguishing between the three diethynylbenzene isomers. At least under jet-cooled conditions, the three isomers are easily distinguished from one another, particularly in the R2PI spectrum. The infrared spectra in the acetylenic C–H stretch region contain characteristic spectral patterns due to Fermi resonance, but these transitions are in such close proximity that distinction on that basis would be difficult.

B. Broad Absorption in S_1 *ortho*-Diethynylbenzene. The most intriguing result of the present work is the broad absorption that appears exclusively in the *ortho*-DEB S_1 -state infrared spectrum. All of the tests outlined in section III.D indicate that the broad absorptions in the S_1 RIDIR spectrum of *o*DEB (Figure 6c) occur out of states that retain their S_1 state character.

The breadth of the absorptions indicates that the upper states accessed with the infrared photon are either very short-lived or very congested (or both). The fact that the absorption is quite localized in frequency ($3050\text{--}3250\text{ cm}^{-1}$) seems inconsistent with directly accessing a repulsive wall of a dissociating state.

It seems more probable that the upper state of this transition is the $S_2(^1B_2)$ state responsible for the vibronic coupling present in the R2PI spectrum. However, we do not understand why this vibronic spectrum is composed of two and only two broadened transitions. One possible scenario would be to assign the two humps in the S_1 infrared spectrum as the $S_1\text{--}S_2$ origin and a low-frequency vibronic band, perhaps ν_{42} , a substituent wagging motion of b_2 symmetry. These bands would be broadened by coupling to other states, which could have diradical character. Similar Franck–Condon factors out of excited vibronic levels would then lead to analogous spectra, as was observed. Although the $S_1\text{--}S_2$ transition is allowed with a transition moment perpendicular to the C_2 axis, the oscillator strength calculated by CIS is quite small ($f = 0.003$). The lack of higher lying vibronic bands would then have to be ascribed to further broadening that hinders their detection.

Mikami and Ebata recently reported the discovery of a “new S_2 ” state in aniline by taking IR spectra in the S_1 state.²⁷ Much like our *o*DEB spectra, broad bands were observed in the spectrum taken out of S_1 which were not present in the same energy region upon UV excitation from the ground state. Two-photon absorption spectra from the ground state revealed the same broad features, which were assigned as vibronic bands of the S_2 state. The $S_0\text{--}S_2$ origin was also located by two-photon absorption although it was not seen in the S_1 infrared spectrum. Such experiments on *o*DEB could confirm the upper state as the $S_2(^1B_2)$ state and determine the origin of this state. However, an initial attempt to do so was unsuccessful.

The fact that the broad bands in the S_1 RIDIR spectrum appear only in the spectrum of the ortho isomer raises the possibility that this absorption is somehow related to the manifold of electronic states of the 1,4-dehydronaphthalene diradical. One anticipates that photochemical routes will be present out of the excited states of *o*DEB that would lead to the diradical. However, very little is known about the excited states of the 1,4-dehydronaphthalene diradical, nor about the pathways connecting the states of the diradical to the ground and excited singlet state levels of *o*DEB. High level ab initio calculations addressing these issues are clearly warranted. In addition, experimental studies of the photochemistry of *o*-diethynylbenzene using wavelengths in the region of the broad absorption could determine if the $S_2(^1B_2)$ state is indeed a gateway to Bergman cyclization.

V. Conclusions

The $S_0\text{--}S_1$ electronic spectra of *ortho*-, *meta*-, and *para*-diethynylbenzene were shown to exhibit a considerable amount of intensity stealing from the nearby S_2 state. Fermi resonance was evident in the ground-state infrared spectra, although it was not present in the overtone of *p*DEB because of C–H stretch anharmonicity or in the S_1 spectra of any isomer because of shifts in the frequencies comprising the combination band. The S_1 infrared spectrum of the ortho isomer was dominated by a broad absorption from 3050 to 3250 cm^{-1} . Persistence of this absorption even in the absence of C–H stretch fundamentals in the spectrum of *o*DEB- d_2 indicated an electronic transition, whereas other tests demonstrated that the absorption showed no dependence on long-lived species. The breadth of the absorption suggests instead a short-lived state, which we propose

may be on the pathway to Bergman cyclization to form the 1,4-dehydronaphthalene diradical.

Acknowledgment. The authors gratefully acknowledge the support of the Department of Energy Basic Energy Sciences, Division of Chemical Sciences under Grant No. DE-FG02-96ER14656 A7. They also acknowledge Dr. Daniel Lee for his synthesis of the *ortho*-diethynylbenzene. J.S. thanks NASA for a Graduate Student Research Fellowship.

References and Notes

- (1) Frenklach, M. *Phys. Chem. Chem. Phys.* **2002**, *4*, 2028.
- (2) Bergman, R. G. *Acc. Chem. Res.* **1973**, *6*, 25.
- (3) Brogli, F.; Heilbronner, E.; Wirz, J.; Kloster-Jensen, E.; Bergman, R. G.; Vollhardt, K. P. C.; Ashe, A. J., III. *Helv. Chim. Acta* **1975**, *58*, 2620.
- (4) King, G. W.; Putten, A. A. G. v. *J. Mol. Spec.* **1978**, *70*.
- (5) Santos Macias, A.; Ballester Reventos, L.; Cano Esquivel, M. *An. Quim.* **1975**, *22*, 47.
- (6) Laposa, J. D. *J. Lumin.* **1979**, *20*, 67.
- (7) Roth, W. R.; Hopf, H. H.; Wasser, T.; Zimmerman, H.; Werner, C. *Liebigs Ann.* **1996**, 1691.
- (8) Prall, M.; Wittkopp, A.; Schreiner, P. R. *J. Phys. Chem. A* **2001**, *105*, 9265.
- (9) Alabugin, I. V.; Manoharan, M.; Kovalenko, S. V. *Org. Lett.* **2002**, *4*, 1119.
- (10) Clark, A. E.; Davidson, E. R.; Zaleski, J. M. *J. Am. Chem. Soc.* **2001**, *123*, 2650.
- (11) Alabugin, I. V.; Manoharan, M. *J. Phys. Chem. A* **2003**, *107*, 3363.
- (12) Evenzahav, A.; Turro, N. J. *J. Am. Chem. Soc.* **1998**, *120*, 1835.
- (13) MacBride, J. A. H.; Wade, K. *Synth. Commun.* **1996**, *26*, 2309.
- (14) Arrington, C. A.; Ramos, C.; Robinson, A. D.; Zwier, T. S. *J. Phys. Chem. A* **1998**, *102*, 3315.
- (15) Page, R. H.; Shen, Y. R.; Lee, Y. T. *J. Chem. Phys.* **1988**, *88*, 4621.
- (16) Omi, T.; Shitomi, H.; Sekipa, N.; Takazawa, K.; Fujii, M. *Chem. Phys. Lett.* **1996**, *252*, 287.
- (17) Frisch, M. J.; Trucks, G. W.; Schlegel, H. B.; Scuseria, G. E.; Robb, M. A.; Cheeseman, J. R.; Zakrzewski, V. G.; Montgomery, J. A., Jr.; Stratmann, R. E.; Burant, J. C.; Dapprich, S.; Millam, J. M.; Daniels, A. D.; Kudin, K. N.; Strain, M. C.; Farkas, O.; Tomasi, J.; Barone, V.; Cossi, M.; Cammi, R.; Mennucci, B.; Pomelli, C.; Adamo, C.; Clifford, S.; Ochterski, J.; Petersson, G. A.; Ayala, P. Y.; Cui, Q.; Morokuma, K.; Malick, D. K.; Rabuck, A. D.; Raghavachari, K.; Foresman, J. B.; Cioslowski, J.; Ortiz, J. V.; Stefanov, B. B.; Liu, G.; Liashenko, A.; Piskorz, P.; Komaromi, I.; Gomperts, R.; Martin, R. L.; Fox, D. J.; Keith, T.; Al-Laham, M. A.; Peng, C. Y.; Nanayakkara, A.; Gonzalez, C.; Challacombe, M.; Gill, P. M. W.; Johnson, B. G.; Chen, W.; Wong, M. W.; Andres, J. L.; Head-Gordon, M.; Replogle, E. S.; Pople, J. A. *Gaussian 98*, revision A.7; Gaussian, Inc.: Pittsburgh, PA, 1998.
- (18) King, G. W.; So, S. P. *J. Mol. Spec.* **1971**, *37*, 543.
- (19) Knight, A. E. W.; Kable, S. H. *J. Chem. Phys.* **1988**, *89*, 7139.
- (20) Ribblett, J. W.; Borst, D. R.; Pratt, D. W. *J. Chem. Phys.* **1999**, *111*, 8454.
- (21) Nguyen, T. V.; Ribblett, J. W.; Pratt, D. W. *Chem. Phys.* **2002**, *283*, 279.
- (22) Swinn, A. K.; Kable, S. H. *J. Mol. Spectrosc.* **1998**, *191*, 49.
- (23) Nyquist, R. A.; Potts, W. J. *Spectrochim. Acta* **1960**, *16*, 419.
- (24) King, G. W.; So, S. P. *J. Mol. Spectrosc.* **1970**, *36*, 468.
- (25) Boyarkin, O. V.; Rizzo, T. R.; Perry, D. S. *J. Chem. Phys.* **1999**, *110*, 11346.
- (26) McEnally, C. S.; Robinson, A. G.; Pfefferle, L. D.; Zwier, T. S. *Combust. Flame* **2000**, *123*, 344.
- (27) Ebata, T.; Minejima, C.; Mikami, N. *J. Phys. Chem. A* **2002**, *106*, 11070.